2019

Tissue resident lymphocytes in human spinal entheses

BOSTON UNIVERSITY

SCHOOL OF MEDICINE

Thesis

TISSUE RESIDENT LYMPHOCYTES IN HUMAN SPINAL ENTHESES

by

MICAH LEFTON

B.S., Northeastern University, 2012

Submitted in partial fulfillment of the

requirements for the degree of

Master of Science

2019

Approved by

First Reader _____

Carl Franzblau, Ph.D.
Professor of Biochemistry

Second Reader _____

Joerg Ermann, M.D.
Assistant Professor of Medicine
Harvard University

TISSUE RESIDENT LYMPHOCYTES IN HUMAN SPINAL ENTHESES

MICAH LEFTON

ABSTRACT

Objective: Ankylosing spondylitis (AS) is an inflammatory disorder within the spondyloarthritis family of rheumatic diseases. AS is characterized by chronic inflammation at entheses, the attachment sites of ligaments or tendons to bone, most prominently in the spine. Chronic enthesitis leads to pathological new bone formation, fusion of vertebral bodies and loss of spinal mobility. Studies in mice identified discrete subsets of enthesis-resident lymphocytes that function within the IL-23/IL-17A signaling pathway and are thought to play a critical role in mediating inflammation and new bone formation. Little is known about such enthesis-resident lymphocytes in humans. The goal of this project was therefore to develop methods to isolate lymphocytes from spinal entheses and analyze them in vitro.

Methods: Cell preparation and staining conditions were optimized using peripheral blood mononuclear cells (PBMCs). We compared surface marker staining of PBMCs exposed to collagenase D, Liberase TL, and dispase II. In addition, we compared the staining of multiple antibody clones specific for CD56 and CD4.

To measure cytokine expression, cells were stimulated with PMA/ionomycin for 4 hours in the presence of monensin and brefeldin A. Following stimulation, the cells were stained with a 17-color staining panel enabling the identification of 8 lymphocyte subsets, 3 killer immunoglobin-like receptors (KIRs), and 4 cytokines implicated in AS pathology. Cell were analyzed on a 5 laser LSRFortessa flow cytometer.

Spine tissue was obtained from laminectomy surgeries performed on patients with degenerative disease of the spine. Interspinous ligament and spinous process bone were cut into 5 mm pieces and cryopreserved in CryoStor CS10, a serum free cryopreservation medium. Samples were stored at -80° C until analysis. After thawing, samples were digested with collagenase D to generate single cell suspensions for analysis by flow cytometry.

Results: Incubation of lymphocytes with collagenases resulted in variable signal attenuation for CD56, CD4, and KIR3DL2. Loss of signal for CD56 occurred with all enzymes and anti-CD56 clones tested but correlated with duration of enzyme exposure. For the anti-CD4 clone OKT4, fluorescence remained stable after digestion. KIR3DL2 signal was lost after incubation with Liberase TL but was not affected by collagenase D.

Spine tissue samples contained the same lymphocyte subsets present in peripheral blood: natural killer (NK) cells, $CD4^+$ T cells, $CD8^+$ T cells, double negative αβ T cells, mucosal-associated invariant T (MAIT) cells, and γδ T cells including vδ1 and vδ2 cells. PMA/ionomycin-stimulated $CD4^+$ T cells from a spine tissue donor had higher fractions of IL-17A and IL-22 positive cells compared to PBMCs from unmatched donors. Granulocyte-macrophage colony-stimulating factor (GM-CSF) production was also increased in spine tissue compared to unmatched PBMCs.

Conclusion: Here we describe an optimized method for releasing lymphocytes from cryopreserved spine tissue specimens with minimal impact on surface marker detection. Similar populations of lymphocytes could be detected in spine tissue and peripheral blood. Stimulation of tissue-resident lymphocytes induced them to produce

inflammatory cytokines. The methods described will be useful to analyze a larger sample size and further characterize the lymphocytes resident to spinal entheses.

TABLE OF CONTENTS

LIST OF TABLES

LIST OF FIGURES

LIST OF ABBREVIATIONS

AF ..... Alexa Fluor

AhR ..... Aryl Hydrocarbon Receptor

APC ..... Allophycocyanine

AS ..... Ankylosing Spondylitis

BSA ..... Bovine Serum Albumin

BUV ..... BD Horizon Brilliant™ Ultraviolet

BV ..... BD Horizon Brilliant™ Violet

CD ..... Cluster of Differentiation

Cy ..... Cyanine

DMEM ..... Dulbecco's Modified Eagle's Medium

EDTA ..... Ethylenediaminetetraacetic Acid

FBS ..... Fetal Bovine Serum

FITC ..... Fluorescein Isothiocyanate

FSC ..... Forward Scatter

FVD ..... Fixable Viability Dye

GM-CSF ..... Granulocyte-Macrophage Colony-Stimulating Factor

HBSS ..... Hanks' Balanced Salt Solution

HEPES ..... 4-(2-hydroxyethyl)-1-piperazineethanesulfonic Acid

HLA ..... Human Leukocyte Antigen

IFNγ ..... Interferon gamma

IMDM ..... Iscove's Modified Dulbecco's Medium

IL ..... Interleukin

ILC ..... Innate Lymphoid Cell

KIR ..... Killer Immunoglobin-Like Receptor

MAIT ..... Mucosal-Associated Invariant T Cell

MFI ..... Median Fluorescent Intensity

MHC ..... Major Histocompatibility Complex

MR-1 ..... MHC Related Protein 1

MRI ..... Magnetic Resonance Imaging

NFAT ..... Nuclear Factor of Activated T Cell

NK ..... Natural Killer

RPMI ..... Roswell Park Memorial Institute Medium

PBMC ..... Peripheral Blood Mononuclear Cell

PE ..... Phycoerythrin

PerCP ..... Peridinin Chlorophyll Protein Complex

PMT ..... Photomultiplier Tube

rSD ..... robust Standard Deviation

SSC ..... Side Scatter

SpA ..... Spondyloarthritis

Tc ..... T Cytotoxic Cell

TCR ..... T Cell Receptor

Th ..... T Helper Cell

INTRODUCTION

Spondyloarthritis (SpA) is a group of inflammatory rheumatic diseases with overlapping clinical features and shared pathophysiology. SpA can be broadly classified as either axial or peripheral SpA, depending on whether the disease predominantly affects the spine or peripheral joints. The prototypical axial SpA is ankylosing spondylitis (AS).[18] AS starts before age 45, with 80% of patients experiencing symptoms prior to the age of 30.[4] The typical AS patient complains about back pain that started insidiously, worsens with rest or during sleep and improves with activity.[19] Chronic inflammation is the likely cause of back pain in AS patients.[19] Some of the earliest detectable inflammation can be seen with magnetic resonance imaging (MRI) of the sacroiliac joints.[19] Radiographic changes such as syndesmophytes, can be seen in the spine as the disease progresses.[19] At late stages, patients experience a permanent loss of spinal mobility as vertebral bodies fuse secondary to formation of bridging syndesmophytes.[19]

Epidemiology

The prevalence of axial SpA in the United States is 0.9-1.4%.[13] Global prevalence varies. The variability of AS prevalence across regions can be largely attributed to genetic factors, particularly a strong association with the gene for Human Leukocyte Antigen B27 (HLA-B27).[15] Different populations around the world have varying frequencies of HLA-B27.[15] In addition, males and females have a different prevalence of AS. While males have historically been diagnosed at higher rates than females, the difference in incidence between males and females has been shrinking in recent years.[5]

This trend is likely the result of new classification criteria and increased use of MRI in diagnosis.[5]

Pathophysiology

IL-23/IL-17A Axis. Immune responses can be globally classified into three major types based on the cytokines involved.[12] One proposed mechanism for the development of AS is activation of a type 3 immune response.[12] It is thought that various forms of stress, such as mechanical, microbial, or cellular, can lead to production of the proinflammatory cytokines IL-1β and IL-23 by stromal and myeloid cells.[9] IL-23 in turn activates lymphocytes expressing retinoic acid receptor-related orphan receptor-γt, a transcription factor that controls the expression of IL-17A.[6,12] These cells include $CD4^+$ T helper 17 (Th17) cells, $CD8^+$ T cytotoxic 17 (Tc17) cells, mucosal-associated invariant T (MAIT) cells, group 3 innate lymphoid cells (ILC3), and some γδ T cells.[12,18] IL-17A promotes inflammation by activating IL-17 receptor-expressing stromal cells. One way IL-17A contributes to AS pathogenesis is by altering the activity of osteoclasts and osteoblasts consequently leading to abnormal bone formation.[9,12]

Other cytokines have also been shown to play a role in AS. IL-22 works with IL-17A to support osteoclastogenesis and is produced by many of the same lymphocytes that make IL-17A.[9,12] GM-CSF is produced by numerous populations of activated lymphocytes.[17] It stimulates progenitors of macrophages and granulocytes to proliferate and its overexpression can lead to severe inflammation.[17] Another important cytokine is interferon γ (IFNγ). IFNγ is primarily released by natural killer (NK) cells, $CD8^+$ T cells,

and Th1 cells in response to intracellular pathogens.[8,9] IFNγ promotes macrophage activity to assist in clearing infected cells.[9]

HLA-B27. The HLA-B27 gene confers the greatest genetic risk for developing AS.[12,15,18] There are multiple hypotheses for how HLA-B27 may contribute to disease. The first concerns the presentation of an arthritogenic peptide.[18] HLA-B27 belongs to the major histocompatibility (MHC) class I family of surface proteins.[12,18] MHC class I proteins are expressed on all cells except red blood cells. They function by binding intracellular peptides and presenting them on the cell surface for recognition by $CD8^+$ T cells.[18] It has been hypothesized that HLA-B27 presents certain arthritogenic peptides thereby driving a $CD8^+$ T cell-mediated immune response.[18] Antigen-experienced cytotoxic T cells are thought to be reactivated in the spine and joints leading to tissue inflammation and disease. Another hypothesis on the relationship of HLA-B27 and AS relates to the intrinsic instability of HLA-B27.[18] Improperly folded HLA-B27 induces an unfolded protein response in the cell causing it to produce proinflammatory cytokines, such as IL-1β and IL-23 in myeloid cells.[12,18] A third hypothesis involves the interaction of HLA-B27 with the receptor KIR3DL2 and other killer-immunoglobulin-like receptor (KIRs). HLA-B27 can abnormally arrange as a heavy chain homodimer lacking β2-microglobulin.[18] HLA-B27 homodimers have been shown to bind KIR3DL2.[12,18]

Killer Immunoglobulin-Like Receptors. KIR3DL2 belongs to the KIR family of receptor types which recognize MHC class I proteins. KIRs are expressed in NK cells, antigen-experienced $CD4^+$ and $CD8^+$ T cells, as well as γδ T cells.[1,8] A KIR is comprised of either two or three extracellular immunoglobin-like domains and a variable length

cytoplasmic domain.[8] Long cytoplasmic domains contain an inhibitory motif whereas short cytoplasmic domains facilitate the interaction with adaptor proteins containing activation motifs.[8] KIR3DL2 is an inhibitory KIR that can bind to HLA-B27 homodimers.[1,8] Expression of KIR3DL2 is significantly increased on NK and Th17 cells in patients with SpA.[1] It has been hypothesized that KIR3DL2 protects NK and Th17 cells from activated-induced apoptosis.[1] In addition, KIR3DL2 expressing NK cells have greater cytotoxic activity and Th17 cells release more IL-17A.[1,14] Th17 cells have also been shown to upregulate expression of KIR3DL2 upon activation.[1,14] This evidence supports a role for the interaction of KIR3DL2 expressing lymphocytes and HLA-B27 homodimers in AS pathogenesis. Another inhibitory KIR, KIR3DL1 binds to properly assembled MHC class I complexes of HLA-B27 heavy chain, peptide and β2 microglobulin.[1,8] However the role of KIR3DL1 involvement in AS is less clear. One study showed no difference in KIR3DL1 expression in healthy patients compared to patients with either SpA or rheumatoid arthritis.[1] A different study hypothesized that NK cells with KIR3DL1 may have reduced cytotoxic capability.[7]

Enthesitis. Inflammation at entheses, the attachment sites of tendons and ligaments to bone, features prominently in SpA pathogenesis and is hypothesized to be the key process driving inflammation in AS.[11] In contrast, synovitis, the primary disease process in rheumatoid arthritis, is thought to be a secondary event in SpA occurring as the result of local cytokine release at inflamed entheses.[11] Mechanical loading of entheses has been shown to activate inflammation and new bone formation.[12,18] Another mechanism of enthesitis involves the IL-23/IL-17A pathway. Overexpression of IL-23 in

a mouse model induced enthesitis at the Achilles tendon insertion.[16] IL-23 responsive cells have recently been found in the enthesis of human spine tissue and have been proposed to play a role in SpA pathogenesis.[2] In vitro stimulation of entheseal spine tissue with IL-1β and IL-23 increased the expression of IL-17A.[2] However, the phenotype of the cells producing IL-17A and other pro-inflammatory cytokines in human entheses has not been fully elucidated.

Objective

The goal of this project was to optimize methods for the isolation of lymphocytes from human spinal entheses and to compare single cell suspensions prepared from spine tissue with peripheral blood lymphocytes using multi-color flow cytometry.

METHODS

Peripheral Blood Mononuclear Cells (PBMC)

Collection. Apharesis leukoreduction collars were obtained from the Brigham and Women's Hospital blood bank and diluted 1:1 in Hanks' Balanced Salt Solution (HBSS) (Corning). Specimens were layered on top of Ficoll-Paque PLUS (GE Healthcare) and centrifuged at 500 g, 20° C, for 30 minutes. The mononuclear cell layer was collected and resuspended in HBSS.

Cryopreservation. PBMCs were centrifuged at 300 g, 4° C, for 10 minutes. Cells were resuspended in fetal bovine serum (FBS) (Gemini) containing 10% dimethyl sulfoxide (Sigma Aldrich) at a density of 10-15 million cells/mL. 1 mL of suspension was transferred to a 1.8 mL cryovial (Thermo Fisher Scientific) and placed in a Mr. Frosty (Thermo Fisher Scientific), an insulated plastic box containing a layer of isopropanol for a controlled rate of cooling (-1° C per minute) in a -80° C freezer. Cryovials were stored at -80° C until use.

In Vitro Stimulation

Cells were resuspended in IMDM-C (Iscove's Modified Dulbecco's Medium (Gibco) supplemented with 10% FBS, 10 mM 4-(2-hydroxyethyl)-1-piperazineethanesulfonic acid (HEPES) (Cellgro), 1 mM sodium pyruvate (Cellgro), 2 mM L-glutamine (Gibco), 1 U/mL penicillin (Sigma Aldrich), 1 μg/mL streptomycin (Sigma Aldrich), nonessential amino acids (Cellgro), and 50 μM 2-mercaptoethanol (Gibco)) and stimulated in a 96-well round-bottom plate with 81 nM phorbol 12-

myristate 13-acetate (PMA) and 134 nM ionomycin (Thermo Fisher Scientific) in the presence of monensin (GolgiStop, BD Bioscience) and brefeldin A (GolgiPlug, BD Bioscience) for 4 hours at 37° C in 5% CO_2.

Flow Cytometry

Staining was performed in 96-well round-bottom plates. Cells were first washed with HBSS and incubated in HBSS containing the Fixable Viability Dye (FVD) eFluor 455UV (Thermo Fisher Scientific) for 15 minutes at 4° C. The Fc receptor was blocked by incubating in Human TrueStain FCX (BioLegend) for 20 minutes at room temperature. For staining of cell surface markers, cells were incubated in staining buffer (HBSS supplemented with 2 μM ethylenediaminetetraacetic acid (EDTA) (Boston BioProducts) and 0.5% bovine serum albumin (BSA) (Sigma Aldrich)) containing antibodies for extracellular proteins as listed in Table 1. Incubation was carried out for 30 minutes at 4° C in the dark. After washes with staining buffer, cells were fixed by incubating in IC Fixation Buffer (Thermo Fisher Scientific) for 15 minutes at room temperature and washed 3 times in Permeabilization Buffer (Thermo Fisher Scientific). Cells were then incubated in Permeabilization Buffer containing antibodies for intracellular targets, as listed in Table 1, for 30 minutes at room temperature in the dark.

After intracellular staining, cells were washed 3 times with Permeabilization Buffer, resuspended in staining buffer, and analyzed on a LSRFortessa (BD Bioscience). The flow cytometer's photomultiplier tubes (PMT) settings were optimized for use with the staining panel, see appendix below.

Color	Marker	Clone	Dilution	Company
BUV395	FVD		1:500	Thermo Fisher
BUV496	CD8	RPA-T8	1:200	BD Bioscience
BV421	MR-1 tetramer	5-OP-RU	1:500	NIH
BV510	αβ TCR	IP26	1:200	BioLegend
BV605	CD4	OKT4	1:200	BioLegend
BV650	IFNγ	4S.B3	1:100	BioLegend
BV711	vδ2 TCR	B6	1:200	BioLegend
BV786	CD56	5.1H11	1:200	BioLegend
FITC	vδ1 TCR	REA173	1:200	BioLegend
PerCP-Cy5.5	KIR3DL1	DX9	1:400	BioLegend
PE	KIR3DL2	DX31	1:500	UCSF
PE-Dazzle	GM-CSF	BVD2-21C11	1:100	BioLegend
PE-Cy5	CD14	61D3	1:500	eBioscience
	CD19	HIB19	1:500	BioLegend
PE-Cy7	IL-22	2G12A41	1:100	BioLegend
APC	KIR3DL1/DS1	Z27	1:100	Beckman Coulter
AF 700	CD3	UCHT1	1:200	BioLegend
APC-Cy7	IL-17A	BL168	1:100	BioLegend

Table 1. Finalized staining panel used for flow cytometry analysis. This panel was modified from one previously used in the lab. IL-22 was added as a parameter, and the clones for CD4 and KIR3DL1/DS1 were exchanged. Antibody dilutions were empirically determined, see appendix below.

Digestive Enzyme and Antibody Clone Selection

We suspended 1.5 x 10^6 PBMCs in 1 mL of Dulbecco's Modified Eagle's Medium (DMEM) (Gibco) supplemented with 0.5% BSA and either 1 mg/mL collagenase D (Roche), 1 mg/mL dispase II (Roche), 0.1 mg/mL Liberase TL (Roche), or

0.5 mg/mL hyaluronidase (Sigma Aldrich). Cells were incubated at 37° C on a shaking table for either 0, 20, 40, or 60 minutes. The cells were then stained for extracellular markers, method described above, and analyzed on a LSRFortessa.

In addition to testing multiple digestive enzymes, we also compared multiple antibody clones for CD4 and CD56 and compared the median fluorescent intensity (MFI) to PBMCs that were incubated without addition of enzymes. 1.5 x 10^6 PBMCs were suspended in 1 mL of DMEM supplemented with 0.5% BSA and either 1 mg/mL collagenase D, 1 mg/mL dispase II, or 0.1 mg/mL Liberase TL. Cells were incubated at 37° C on a shaking table for 60 minutes. The cells were then stained for extracellular markers. For CD56, the clone used was either 5.1H11, HCD56, MEM188, or QA17A16. For CD4, the clone was either RPAT4, SK3, or OKT4.

Lastly, as no alternative antibody clones were available for KIR3DL2, we examined if KIR3DL2 fluorescence would recover by allowing cells to rest after digestion. 1.5 x 10^6 PBMCs were incubated in DMEM, 0.5% BSA with either 1 mg/mL collagenase D or 0.1 mg/mL Liberase TL at 37° C for 40 minutes. Cells were washed and analyzed either immediately or after resting in RPMI-C (Roswell Park Memorial Institute medium (Gibco) supplemented as described for IMDM-C) at 37° C for 4 or 12 hours.

Spine Tissue

Collection. Discarded lumbar spinous process bone and interspinous ligament specimens were obtained from non-AS patients undergoing surgical laminectomy for spinal decompression (Figure 1). Specimens were obtained from the Department of

Orthopedic Surgery at Brigham and Women's Hospital and Brigham and Women's Faulkner Hospital. Following surgery, tissue was transported in sterile normal saline and immediately processed. Tissue was rinsed in HBSS and remained submerged in HBSS throughout processing. Using scissors, soft tissue was cut away from the spinous process. The bone was cut transversely with shears and cut again along its sagittal plane (Figure 1). Most of the marrow and trabecular bone was cleared away. Bone was then cut into 5 mm diameter pieces for analysis. Interspinous ligament adjacent to bone was cut into less than 5 mm pieces using scissors (Figure 1).

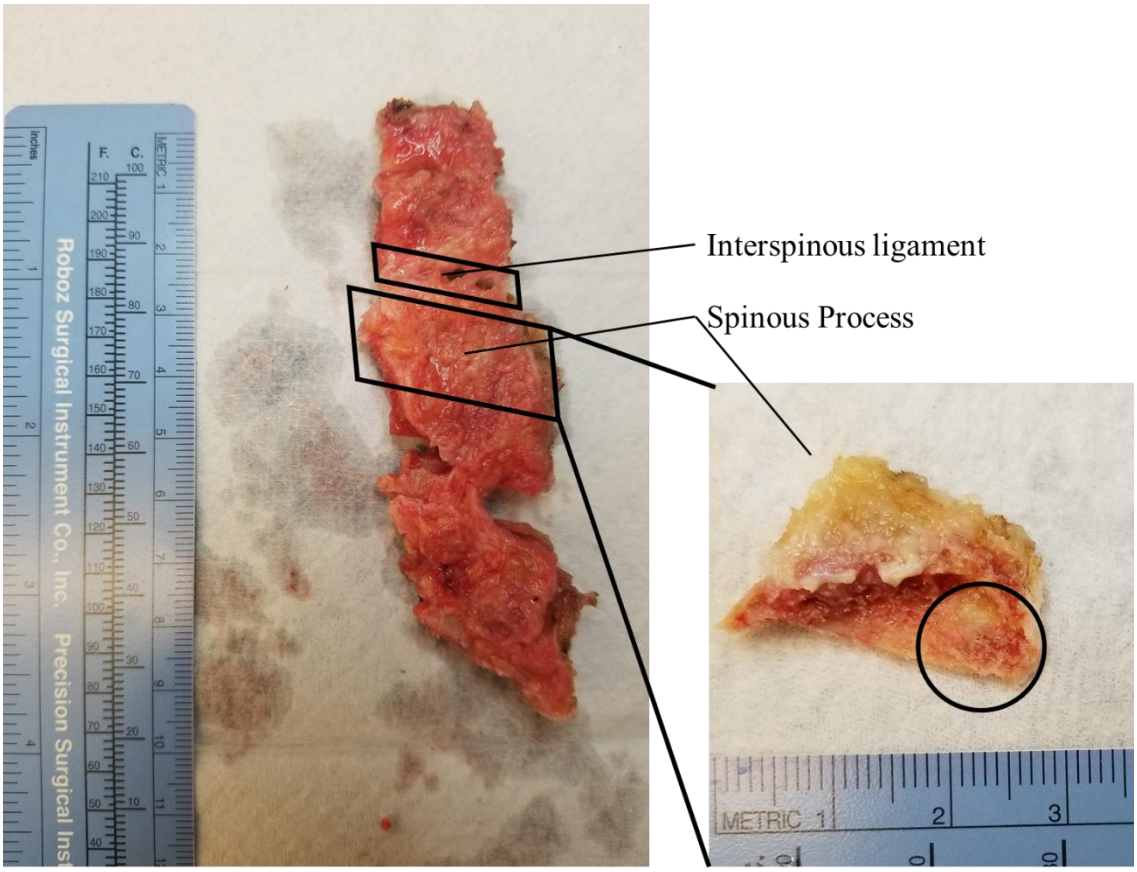

Figure 1. Left: Spinous process L2 through L5 from a laminectomy surgery. The interspinous ligament in the outlined selection was dissected for analysis. **Right:** Spinous process after removal of the surrounding soft tissue. The bone was first transversely cut in half and then

dissected along the sagittal plane to approximate mid-point. The circled section was removed for analysis.

Cryopreservation. Ligament or bone tissue pieces were added to 1 mL of CryoStor CS10 (BioLife Solutions) in a cryovial until the final volume reached 1.5 mL. Cryovials were frozen as described above and stored at -80° C.

Enzymatic Digestion. Frozen tissue samples were thawed by manually stirring the cryovial in a 37° C water bath. After thawing, the tissues pieces were removed from the cryovial, rinsed with DMEM supplemented with 0.5% BSA and then placed in 2.5 mL of DMEM with 0.5% BSA, 1 mg/mL collagenase D (Sigma Aldrich), and 100 μg/mL DNase I (Sigma Aldrich). Interspinous ligament specimens were further minced with scissors. Samples were incubated for 40 minutes at 37° C on a shaking table. Following digestion, the tissue was ground through a 70 μm cell strainer and washed with RPMI-C.

Flow cytometry and Statistical Analysis

Analysis of flow cytometry data was done using FlowJo V10.5.3. Statistical analysis and graphing were performed using GraphPad Prism 7. *P* values were calculated using the paired or unpaired Student's *t* test. *P* values less than 0.05 were considered significant.

RESULTS

Flow Cytometry Gating Strategy

The flow cytometry staining panel (Table 1), modified from a staining panel previously developed in the lab, can identify 8 lymphocyte populations, explained below, as well as the receptors KIR3DL2, KIR3DL1, KIR3DS1, and the cytokines IL-17A, IL-22, GM-CSF, and IFNγ. Figure 2 shows the gating strategy on a representative example of PBMCs from a healthy individual. Lymphocytes are gated based on forward scatter (FSC) and side scatter (SSC), and doublets are excluded. FVD^+ non-viable cells, $CD14^+$ monocytes and $CD19^+$ B cells are excluded. Next, NK cells are identified as $CD3^-$ $CD56^+$ cells. $CD3^+$ T cells are then separated into αβ T cell receptor positive and negative fractions. $CD3^+\alpha\beta TCR^-$ cells represent γδ T cells and can be distinguished further as vδ1 cells, vδ2 cells, or other γδ T cells. MAIT cells are identified as $CD3^+\alpha\beta TCR^+MR1^+$. $CD3^+\alpha\beta TCR^+MR1^-$ cells are separated based on expression of CD4 and CD8 into $CD4^+$ T cells, $CD8^+$ T cells and $CD4^-CD8^-$ DN αβ T cells. These lymphocyte subsets can then be analyzed for expression of KIRs or induction of cytokines upon stimulation with PMA/ionomycin.

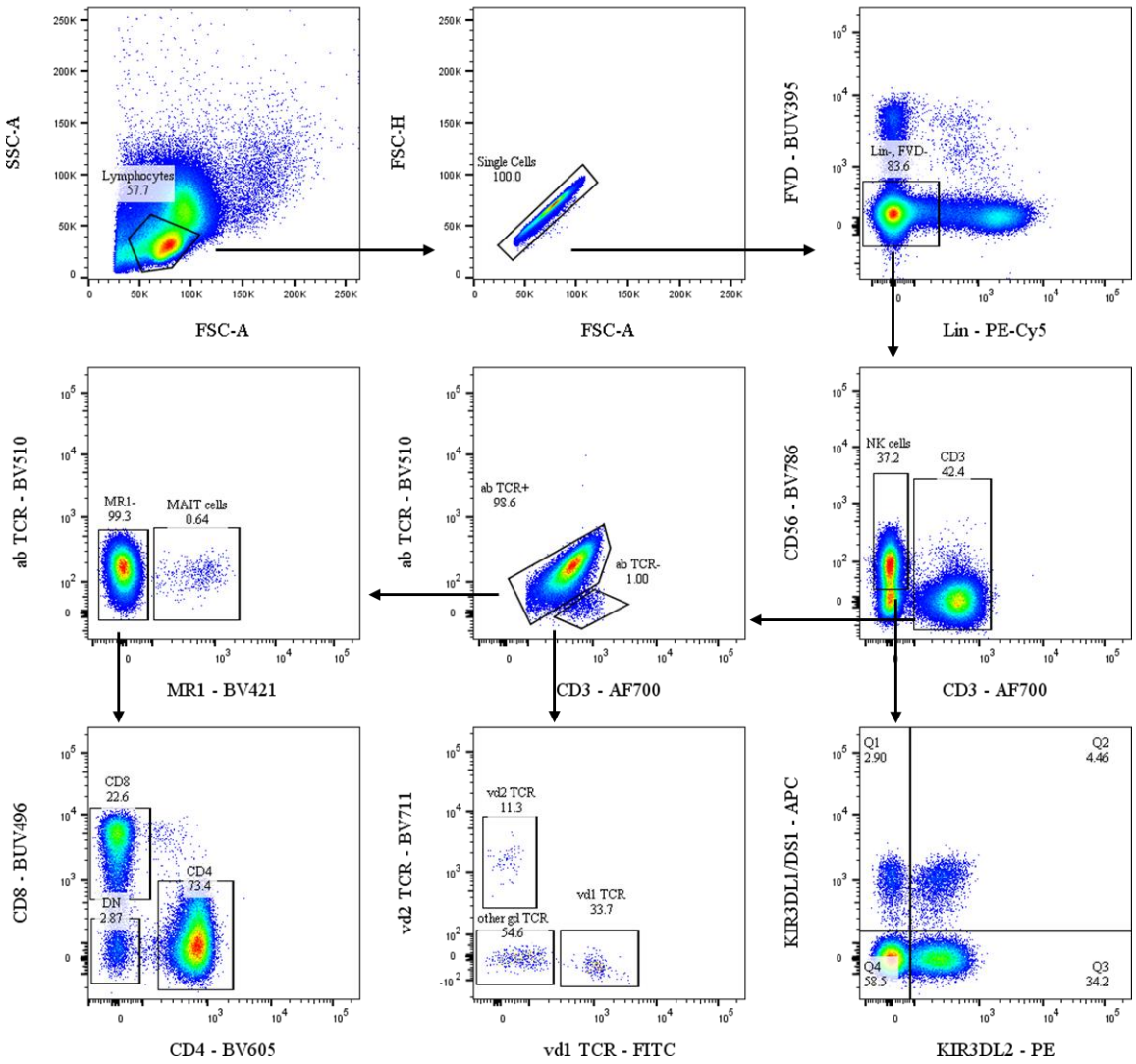

Figure 2. Flow cytometry gating strategy on a sample of PBMCs from a healthy donor to identify 8 lymphocytes populations: NK Cells (middle right), MAIT cells (middle left), $CD4^+$ T cells (bottom left), $CD8^+$ T cells (bottom left), DN αβ T cells (bottom left), vδ1 T cells (bottom middle), vδ2 T cells (bottom middle), and other γδ T cells (bottom middle).

Digestive Enzymes and Antibody Clones

To test the conditions for lymphocyte isolation from spine tissue, we incubated PBMCs with digestive enzymes followed by flow cytometric analysis for cells surface markers using the panel described above. While most markers were unaffected by

enzymatic digestions, we observed significant effects on CD56, CD4, and KIR3DL2 signals. The CD56 MFI gradually decreased over time in collagenase D, Liberase TL, and in dispase II (Figure 3). Hyaluronidase did not affect CD56 staining (not shown). The CD4 signal was rapidly lost upon incubation with dispase II and Liberase TL (Figure 4). There was a mild decrease in CD4 staining after incubation in collagenase D (Figure 4), and hyaluronidase had no effect (not shown). In summary, incubation of PBMCs in digestive enzymes reduced the MFI of key surface markers. We next examined whether modifications of the digestion and staining protocol would mitigate these unwanted surface marker changes.

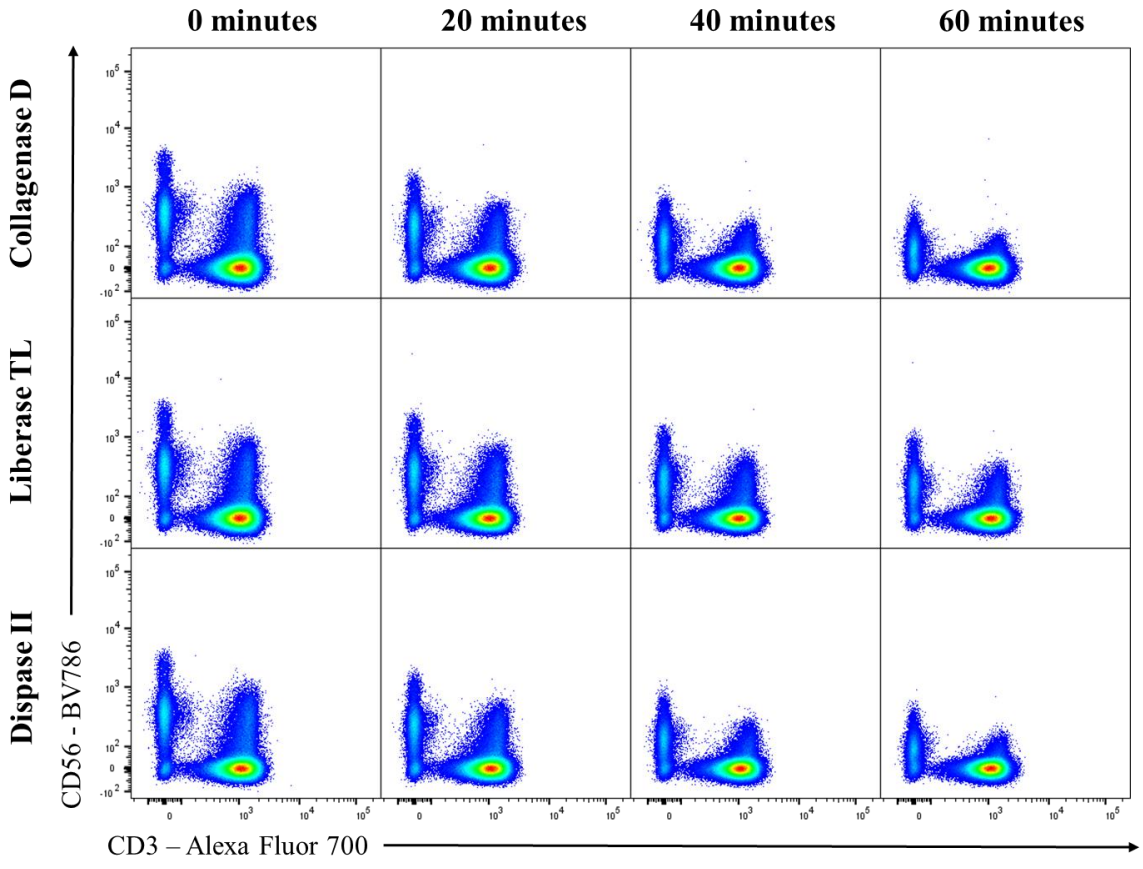

Figure 3. PBMCs were incubated in digestive enzyme for 0, 20, 40, 60 minutes at 37° C. Cells were then analyzed by flow cytometry. Displayed are viable lymphocytes (middle right panel in

Figure 2). With increased exposure time to each of the enzymes, the MFI of CD56 gradually decreased while the CD3 signals remained unchanged.

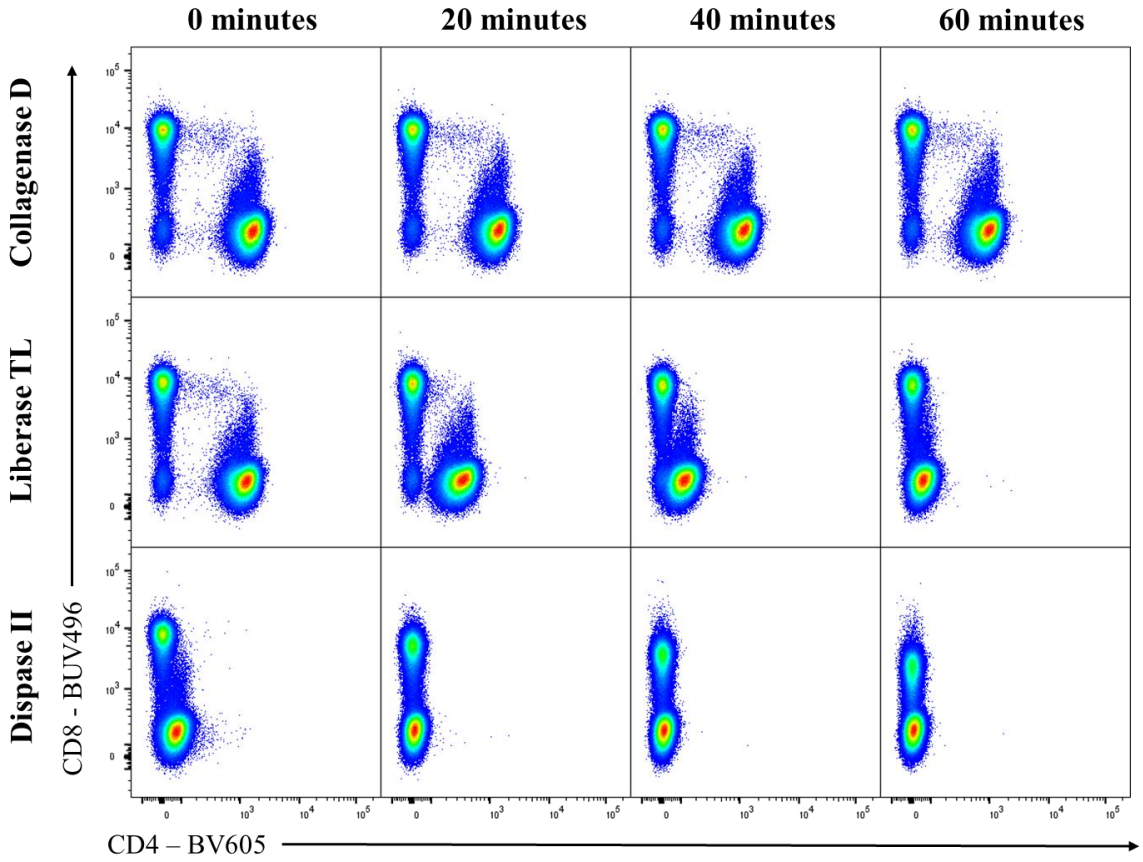

Figure 4. PBMCs were incubated in digestive enzyme for 0, 20, 40, 60 minutes at 37° C. Cells were then analyzed by flow cytometry. Displayed are $CD3^{+}\alpha\beta TCR^{+}$ cells (bottom left panel in Figure 2). MFI of CD4 with small decrease over time in collagenase D, a moderate decrease in Liberase TL, and a rapid and complete loss of signal in dispase II.

We tested the use of different antibody clones for CD56 and CD4 reasoning that enzymatic digestion might destroy the epitopes of some anti-CD56 and anti-CD4 antibodies but not others. We tested 4 different clones for CD56 (5.1H11, HCD56, MEM188, QA17A16) and 3 different clones for CD4 (RPAT4, SK3, OKT4) in order to identify clones specific for more stable epitopes. Overall, while none of the clones we tested for CD56 were able to maintain fluorescent signal following enzyme digestion

compared to control, Liberase TL had less of an effect than collagenase D (Figure 5). For CD4, the OKT4 clone was not affected by Liberase TL or collagenase D digestion (Figure 6).

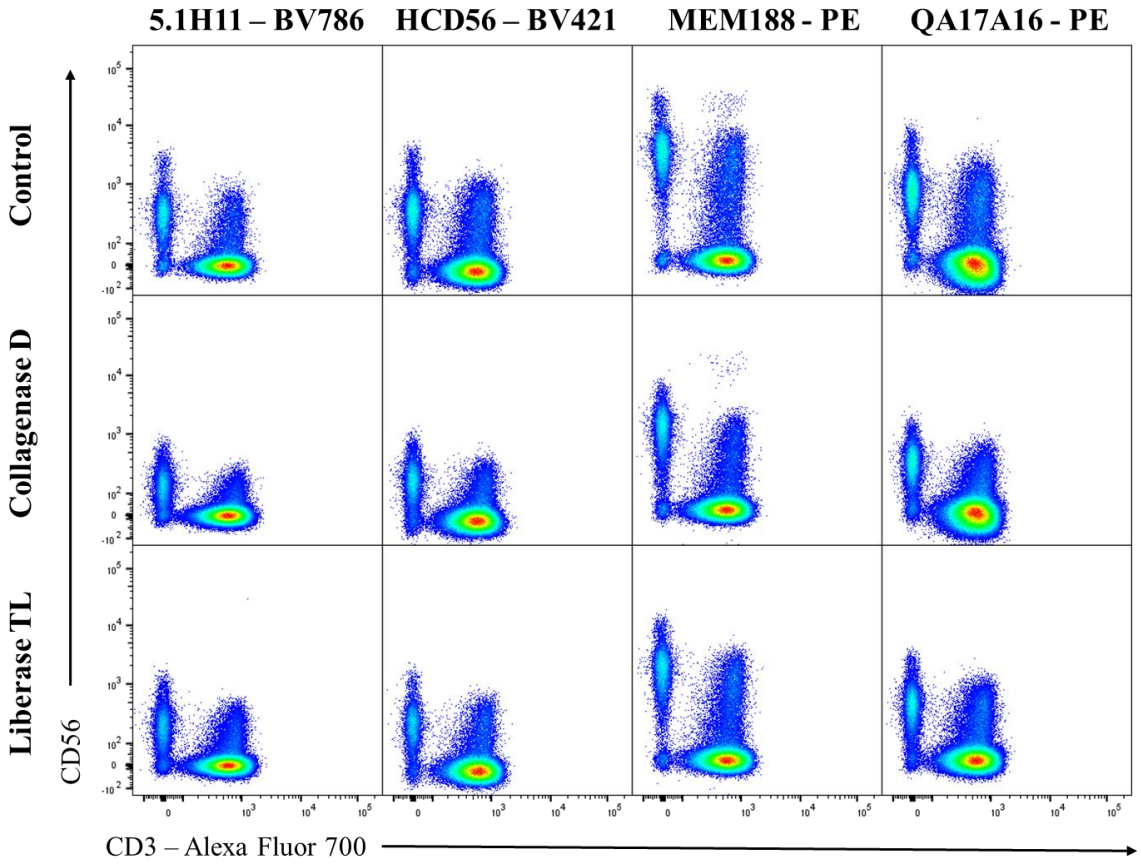

Figure 5. PBMCs were incubated in digestive enzyme for 60 minutes at 37° C. Cells were stained with different antibody clones for CD56 and then analyzed by flow cytometry. Displayed are viable lymphocytes (middle right panel in Figure 2). The MFI for all clones decreased following digestion compared to control.

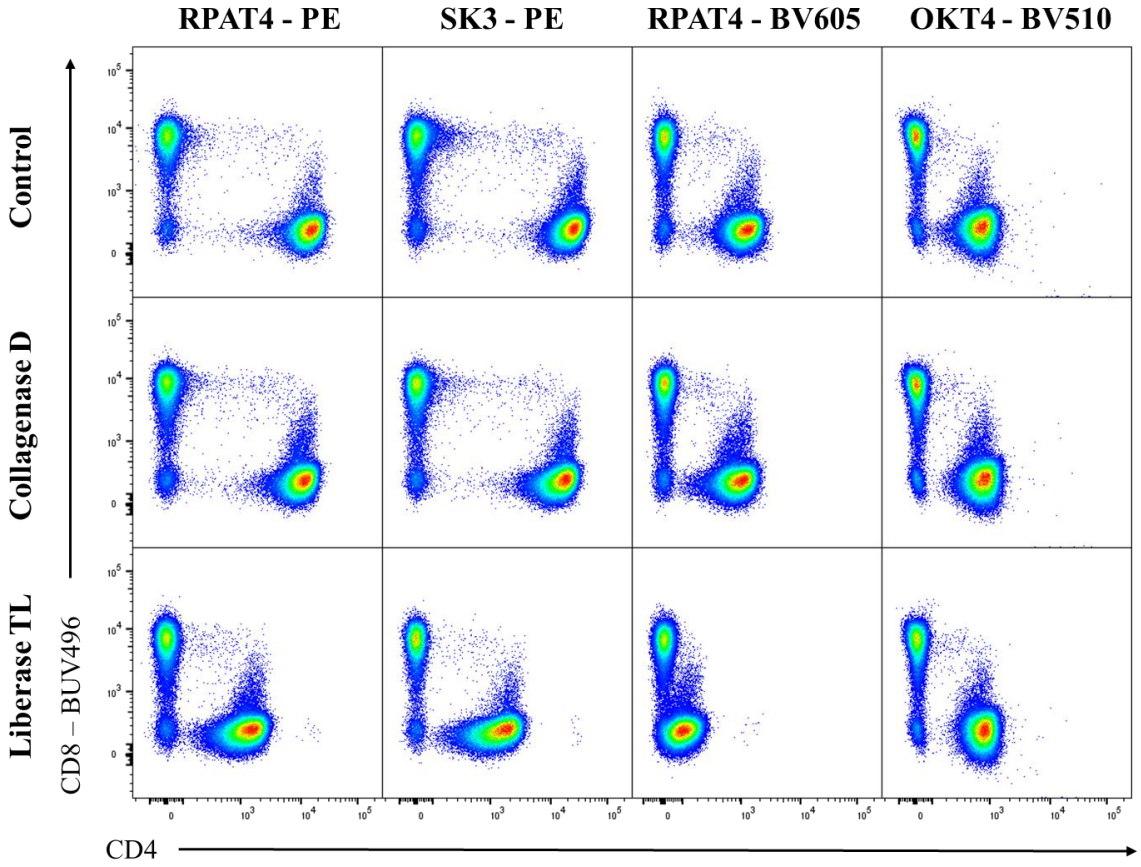

Figure 6. PBMCs were incubated in digestive enzyme for 60 minutes at 37° C. Cells were stained with different antibody clones for CD4 and then analyzed by flow cytometry. Displayed are $CD3^{+}\alpha\beta TCR^{+}$ cells (bottom left panel in Figure 2). There was a decrease in CD4 MFI in digested PBMCs after staining with either the RPAT4 or SK3 clone. There was no change in CD4 MFI for PBMCs stained with the OKT4 clone.

KIR3DL2 fluorescence was not affected by collagenase D while Liberase TL completely eliminated staining for KIR3DL2. We attempted to rescue the KIR3DL2 signal by allowing cells to rest prior to flow cytometry analysis. Figure 7 shows that there was incomplete recovery of KIR3DL2 signal after resting the cells for 4 or 12 hours, respectively.

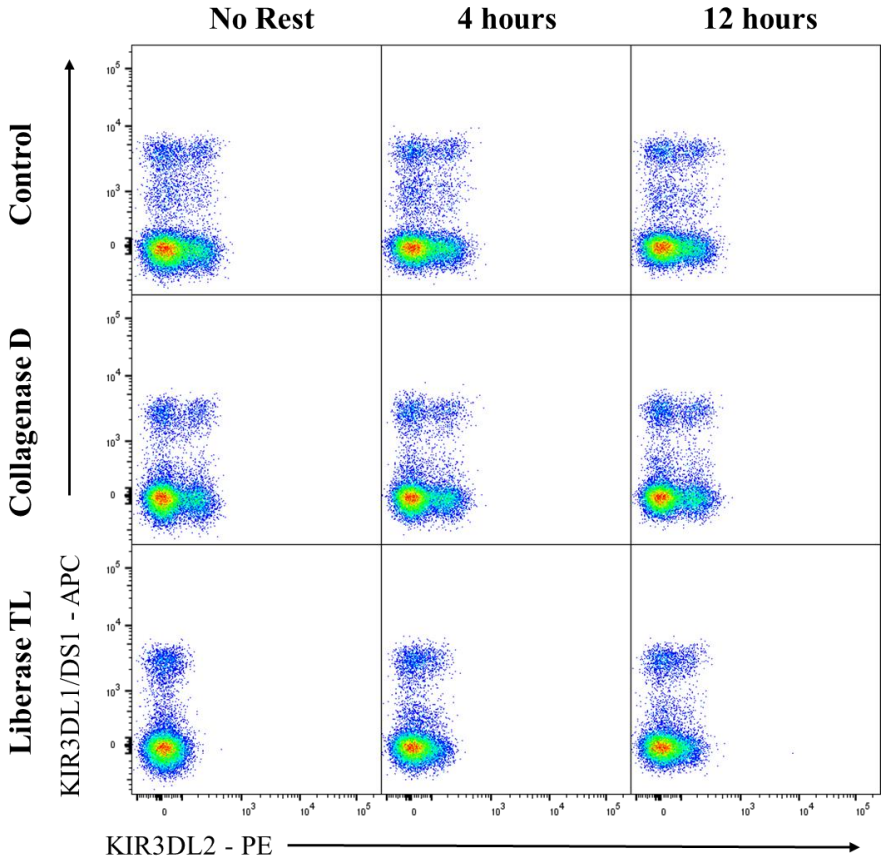

Figure 7. PBMCs were incubated in digestive enzyme for 40 minutes at 37° C. Cells were analyzed by flow cytometry either immediately, after a 4-hour rest in RPMI-C at 37° C, or after a 12-hour rest. Displayed are NK cells (bottom right panel in Figure 2). The KIR3DL2 signal was eliminated after digestion with Liberase TL. There was minimal recovery of signal after resting the cells for 4 or 12 hours. No change in KIR3DL2 signal following collagenase D digestion.

Based on these results, the following adjustments were made to the digestion and staining protocol: (I) Collagenase D was selected as the digestive enzyme. While it caused a slightly greater loss of CD56 signal compared with Liberase TL, collagenase D did not alter KIR3DL2 staining (Table 2). (II) An incubation time of 40 minutes was selected to balance digestive activity to release lymphocytes with maintaining the CD56 signal. (III) The OKT4 clone was selected for detecting CD4 as OKT4 staining was not impacted by collagenase digestion (Figure 8).

	CD56	CD4	KIR3DL2
Control	No Change	No Change	No Change
Collagenase D	↓↓	↓	No Change
Liberase TL	↓	↓↓↓	↓↓↓
Dispase II	↓↓	↓↓↓	↓↓
Hyaluronidase	No Change	No Change	No Change

Table 2. Summary of how each digestive enzyme altered the MFI for select surface markers. RPAT4 used to stain CD4.

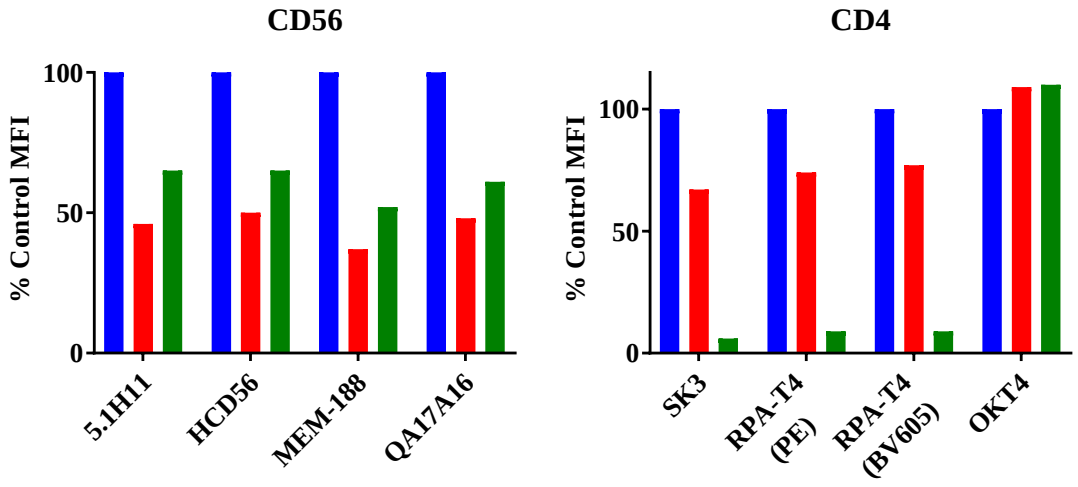

Figure 8. Change in MFI of CD56 (left) and CD4 (right) after staining with each clone. PBMCs were digested in either collagenase D (red) or Liberase TL (green) for 1 hour at 37° C. PBMCs stained without being digested (blue) represented 100% MFI. CD4 MFI of PBMCs stained with OKT4 had no decrease with digestion.

Detection of Spinal Enthesis Resident Lymphocytes

When applied to spine tissue, the digestive enzyme protocol released lymphocytes from connective tissue and enabled analysis by flow cytometry. The described staining panel and gating strategy enabled the detection of lymphocyte populations in the

interspinous ligament (Figure 9) and spinous process (Figure 10) similar to those found in PBMCs (Figure 2).

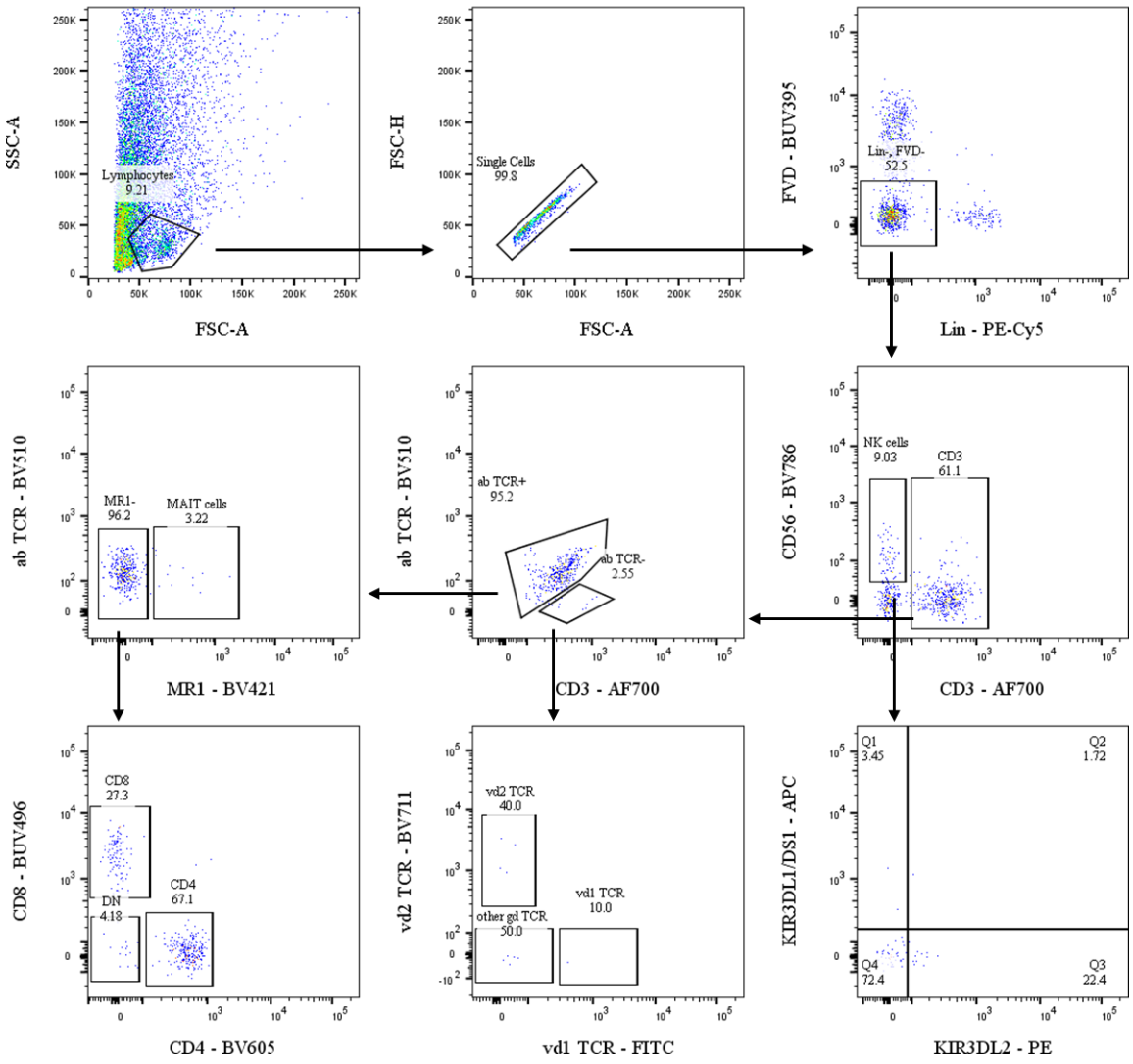

Figure 9. Lymphocytes from the interspinous ligament were isolated using digestive method as described. Single cell suspensions were then analyzed by flow cytometry, lymphocyte populations were gated using the same strategy described in Figure 2.

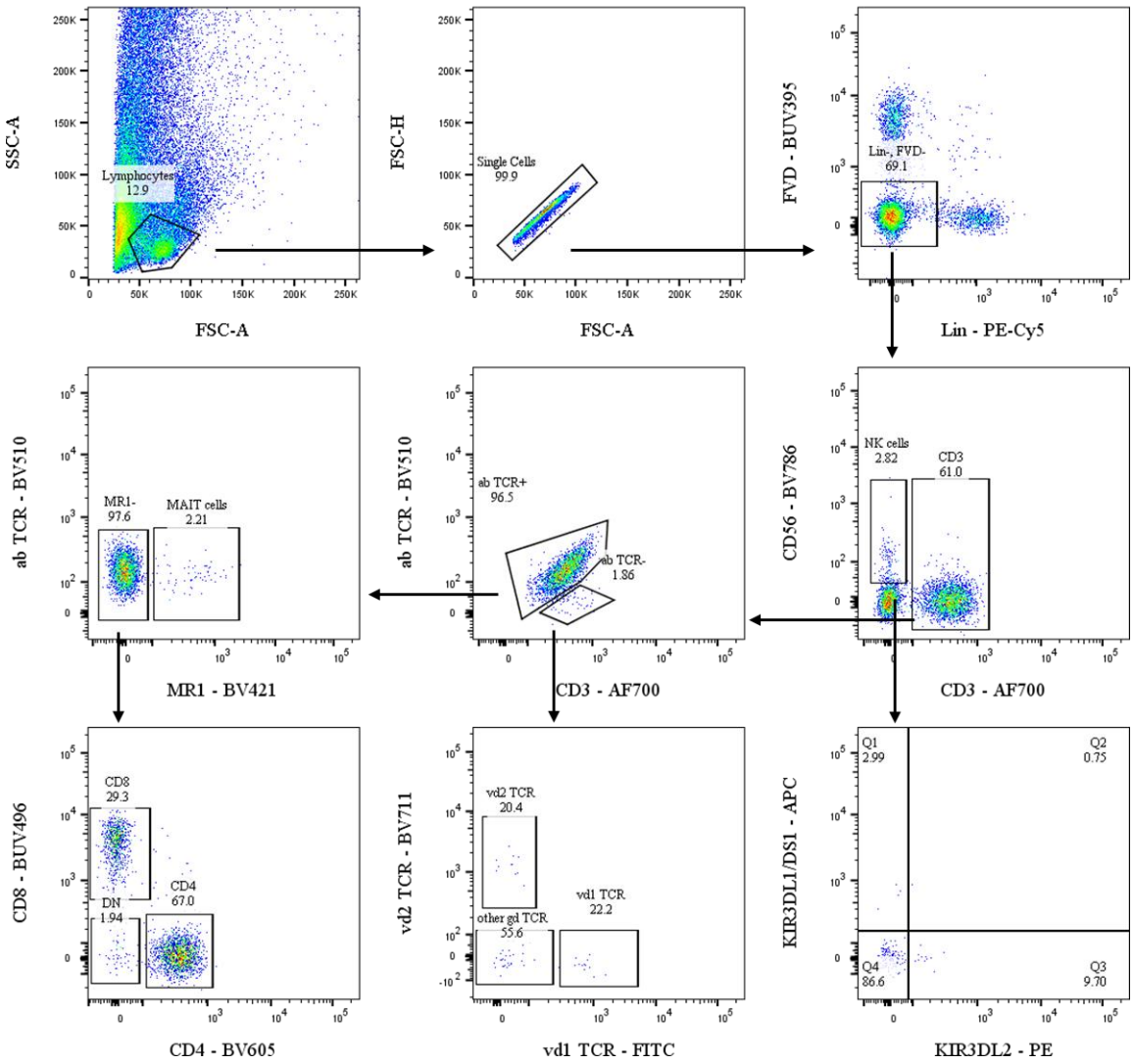

Figure 10. Lymphocytes from the spinous process were isolated using digestive method as described. Single cell suspensions were then analyzed by flow cytometry, lymphocyte populations were gated using the same strategy described in Figure 2.

The staining panel and gating strategy enabled identification of NK cells, $CD4^+$ T cells, $CD8^+$ T cells, double negative αβ T cells, MAIT cells, vδ1 T cells, vδ2 T cells, and other γδ T cells in both the interspinous ligament and spinous process bone.

Stimulation of Spinal Enthesis Resident Lymphocytes

Next, lymphocytes isolated from interspinous ligament and spinous process were activated in vitro by stimulation with PMA/ionomycin for 4 hours. All detectable lymphocyte populations stained positive for the cytokines IFNγ and GM-CSF (Figure 11). $CD4^+$ T cells additionally were positive for IL-17A and IL-22 (Figure 12). MAIT cells were also positive for IL-17A (not shown).

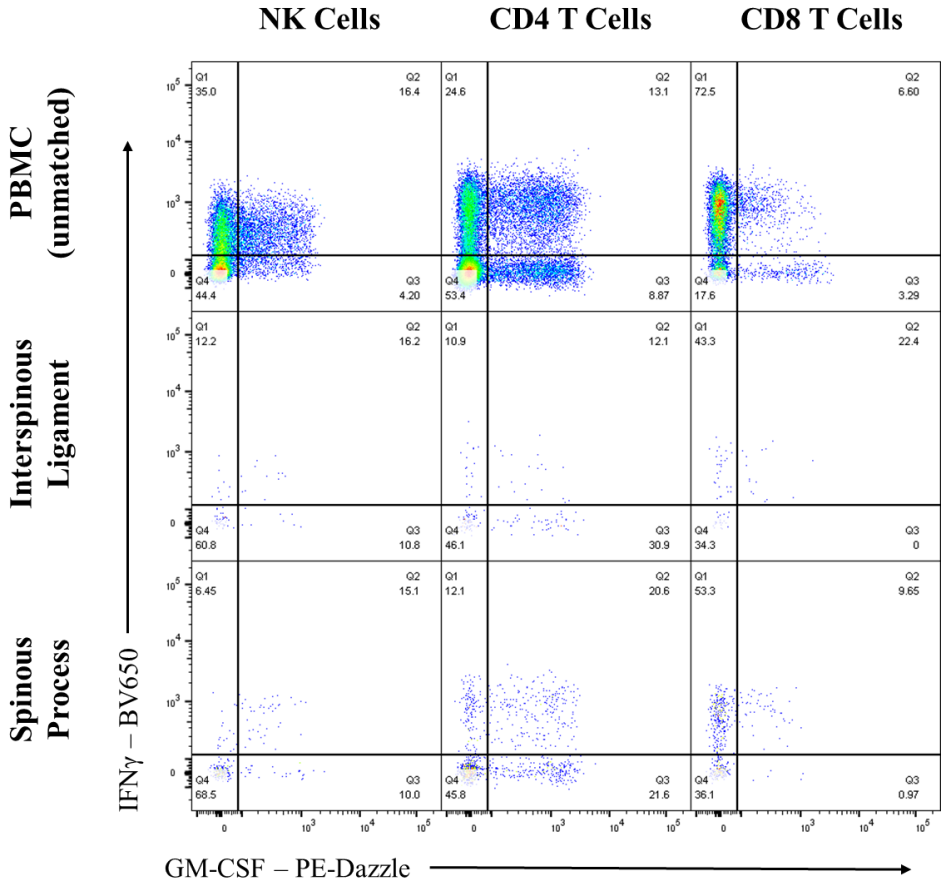

Figure 11. Lymphocytes from peripheral blood or isolated from spine tissue were stimulated with PMA/ionomycin for 4 hours at 37° C. Lymphocyte populations were gated using the same strategy described in Figure 2. GM-CSF and IFNg production are shown for NK cells, $CD4^+$ T cells, and $CD8^+$ T cells.

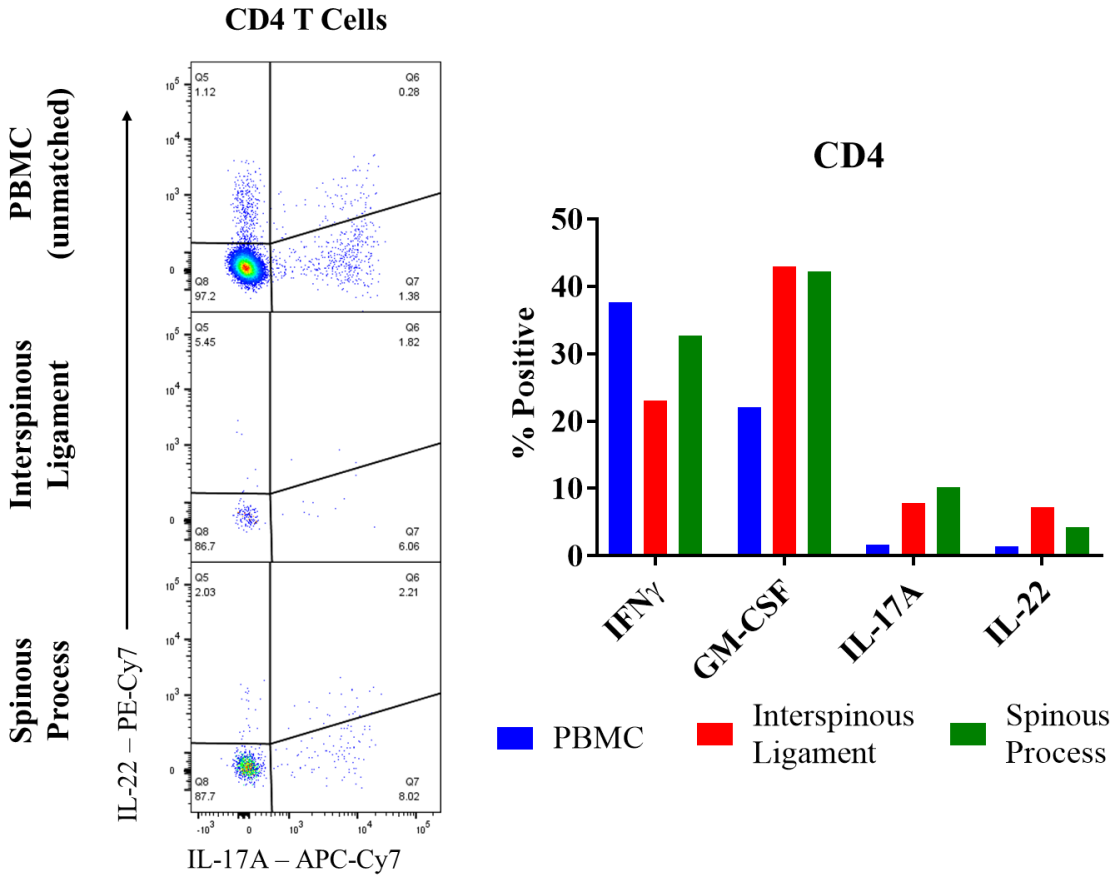

Figure 12. Lymphocytes from peripheral blood or isolated from spine tissue were stimulated with PMA/ionomycin for 4 hours at 37° C. **Left:** Lymphocyte populations were gated using the same strategy described in Figure 2. $CD4^+$ T cells were positive for IL-17A and IL-22. **Right:** Percent of $CD4^+$ cells positive for each cytokine from either PBMCs, interspinous ligament, or spinous process bone.

When compared to an unmatched sample of PBMCs, lymphocytes isolated from spine tissue appeared to exhibit differences in cytokine. The $CD4^+$ T cells from the spine had lower fractions of IFNγ producing cells and higher fractions of GM-CSF, IL-17A, and IL-22 producing cells compared to unmatched PBMCs (Figure 12).

DISCUSSION

We were able to isolate tissue resident lymphocytes from the interspinous ligament and spinous process bone from patients with degenerative disease and analyze the cells by flow cytometry using a 17-color panel previously developed for the analysis of peripheral blood lymphocytes. We were able to detect the same lymphocyte populations identified in peripheral blood, namely NK cells, $CD4^+$ helper T cells, $CD8^+$ cytotoxic T cells, double negative αβ T cells, MAIT cells and γδ T cells. Moreover, secretion of the AS relevant cytokines IL-17A, IL-22, IFNγ and GM-CSF could be demonstrated upon short-term stimulation with PMA/ionomycin in vitro.

We observed significant changes in extracellular protein levels when analyzed by flow cytometry after exposure to digestive enzymes. Of the surface markers included in our staining panel, KIR3DL2, CD4, and CD56 were susceptible to signal loss after incubation with digestive enzymes. This was likely the result of enzymatic cleavage of peptide bonds leading to conformational changes that prevented the fluorochrome-labeled antibodies from binding to their epitopes.

We found some solutions to mitigate the changes that occurred. Alternative clones were available for CD56 and CD4. We found that one anti-CD4 clone (OKT4) identified its target regardless of exposure to digestive enzymes. Determining the optimal digestive enzyme also helped. We compared two collagenase preparations, Liberase TL and collagenase D, and found that they had different effects on surface protein levels. The CD56 signal decreased less in Liberase TL than in collagenase D. In contrast, KIR3DL2 staining was eliminated by Liberase TL while it was not changed by collagenase D. As

Liberase TL was less detrimental to CD56, we attempted to recover the KIR3DL2 signal by allowing cells to rest following incubation in Liberase TL. However, even after 12 hours of incubation, there was only partial return of the KIR3DL2 signal. While allowing the cells to rest longer may further improve signal recovery, we are concerned that prolonged incubation might confound the data by decreasing cell viability and artificially selecting some cell populations over others. Selecting appropriate digestive enzymes and flow cytometry antibody clones is critical when attempting to characterize cells isolated from tissue.

We also examined the feasibility of cryopreserving tissue prior to generating single cell suspensions. Cryopreservation has been demonstrated to be effective in preserving PBMCs and certain cell types in synovial tissue.[3] We compared lymphocyte subsets analyzed from fresh spinous process bone to matched tissue that was stored at -80° C for 14 days in a commercial freezing medium, CryoStor CS10. Cells prepared and analyzed after cryopreservation showed no differences in flow cytometry staining patterns or frequency of several lymphocyte subsets compared to cells prepared and analyzed on the day of surgery (see appendix).

Cryopreservation has the potential to be highly useful in this research. Our means of obtaining spinal tissue rely on patients undergoing spine surgery. These surgeries may occur at hours that make immediate tissue processing and analysis impractical. Having the ability to quickly preserve tissue for later processing relieves this problem. Moreover, tissue samples can be obtained from multiple clinical sites thereby increasing the potential pool of donors and permitting centralized tissue processing and analysis. Tissue

can also be stored until a sufficient sample size is obtained and processed in parallel to reduce batch effects.

As additional work is done and more data are collected, it is necessary for studies to clearly specify the experimental design. We observed differences in cytokine production from the same cells after stimulation with PMA/ionomycin in different types of media (see appendix). More cells stained cytokine-positive when stimulated in IMDM compared to the commonly used RPMI. Another potential source of variability between studies is the precise location of the tissue dissected for enzymatic digestion. In this study, we used tissue from laminectomy surgeries. While preparing the interspinous ligament for cell isolation was straightforward, selecting a defined bone sample proved to be quite complicated. Bone pieces were surrounded by soft tissue, which could not be completely removed prior to tissue digestion. In addition, bone marrow cells were likely included that may not be representative true entheseal cells. A previous study that examined spine tissue referred to peri-entheseal bone as a region distinct from entheseal soft tissue.[2] However, the group did not specify how they determined the peri-entheseal region and if it included bone marrow or adjacent soft tissue. While inclusion of multiple cell sources does not invalidate the data, specifying the tissue origin of resident lymphocytes is important for drawing conclusions and making consistent comparisons.

This study had a number of weaknesses. Few cells were obtained from the spine tissue after digestion. Only 392 $CD3^+$ cells from the interspinous ligament sample were evaluated on the flow cytometer. 2,900 $CD3^+$ cells were isolated from the spinous process, which likely included cells from the bone marrow as well as the enthesis. For

comparison, the PBMC data set included nearly 64,000 $CD3^+$ cells. Several of the lymphocyte subsets included in our staining panel represent less than 5% of the total cell population. A higher number of analyzed events will improve the accuracy of quantifying cell populations with such low frequency.

Another limitation is the lack of matched samples from the spine and peripheral blood of the same patients. However, the primary objective of this study was to optimize methods and demonstrate feasibility of analyzing lymphocytes from spine tissue. Obtaining matched specimens from spine and peripheral blood will be important for future studies. Identifying what types of lymphocytes are present at the spinal enthesis is a necessary first step for understanding the pathogenesis of AS. While our findings clearly demonstrate immune reactivity in spine tissue, these results are only preliminary and qualitative. Increasing the sample size of analyzed tissues will be an important next step. Individuals have inherently large variations in lymphocyte fractions. Factors such as genetics and medical history may contribute to differences between individuals. As more tissue samples are examined, additional variables can be measured. These methods could specifically be used to identify HLA-B27 binding KIRs on tissue resident lymphocytes. While we did not collect genetic information in this study, future work could easily be expanded to include data such as HLA-B27 and compare cells isolated from the spine of $HLA\text{-}B27^+$ and $HLA\text{-}B27^-$ individuals. Ultimately, one would like to compare cells from patients with AS with non-AS patients. These types of studies will improve our understanding AS pathogenesis and open new opportunities for treatment.

APPENDIX

Photomultiplier Tube (PMT) Voltage Optimization

In the flow cytometer, photons emitted from excited fluorochromes are filtered to specific PMTs based on their wavelength. Photons hitting the PMT are amplified across a series of dynodes to generate an electrical current that is proportional to the number of photons. The flow cytometry software reads the current as a measurement of the cell's fluorescent intensity. Users can modify the voltage of the PMT to optimize the level of signal amplification. If the voltage is too low, the user will be unable to distinguish positive from negative signals. If the voltage is too high, electrical noise is introduced (Figure A2). Optimal voltage settings maximize the separation between positive and negative signals while minimizing noise.[10] We determined the PMT settings on our flow cytometer by calculating the stain index over a range of voltages for each color used in our staining panel.

UltraComp eBeads (Thermo Fisher Scientific) were diluted 1:20 in staining buffer. Beads were incubated separately with each antibody from the flow cytometry panel in Table 1 at a 1:500 dilution for 30 minutes at 4° C. Following incubation, beads were analyzed on a LSRFortessa using 8 different PMT voltage settings in 50 mV increments. MFI of positive and negative populations as well as robust standard deviation (rSD) of the negative population were calculated using FlowJo. and the stain index was calculated at each voltage using the equation in Figure A1. Voltages selected for use are listed in Table A1.

$$Stain\ Index = \frac{MFI\ positive - MFI\ negative}{2 \times rSD\ negative}$$

Figure A1. Stain index calculation.[10]

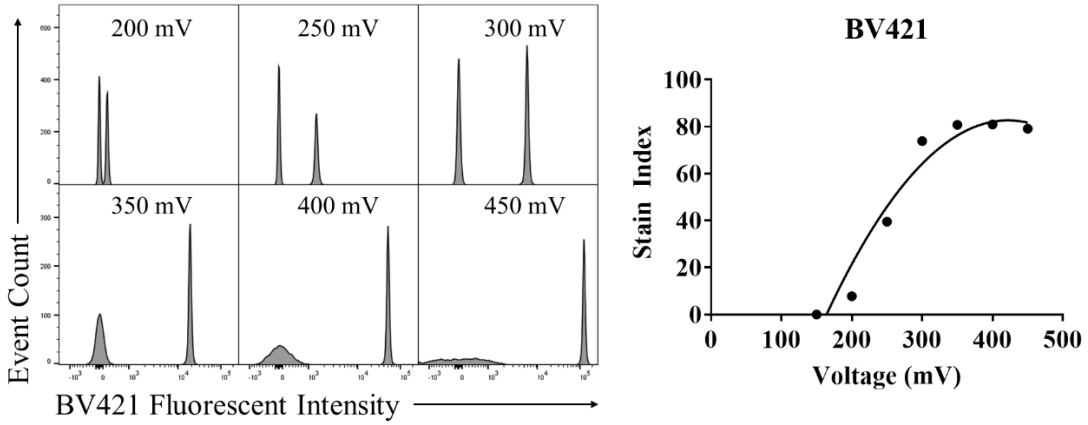

Figure A2. Left: Histogram plots showing signal intensity and separation between unstained beads and beads stained with a BV421-labeled antibody. Data were collected for the same sample using PMT voltages between 200 mV and 450 mV. **Right:** Stain index of BV421 over 50 mV increments.

Color	Voltage (mV)	Color	Voltage (mV)
BUV395	450	PerCP-Cy5.5	550
BUV496	450	PE	500
BV421	350	PE-Dazzle	350
BV510	400	PE-Cy5	475
BV605	450	PE-Cy7	500
BV650	450	APC	550
BV711	475	Alexa Fluor 700	450
BV786	475	APC-Cy7	550
FITC	450		

Table A1. Optimized PMT voltages.

Antibody Dilution Titration

IL-17A and IL-22. 5 wells with approximately 1.5 x 10^6 PBMCs each were stimulated with PMA/ionomycin and stained extracellularly and intracellularly as described in methods. The IL-17A and IL-22 antibody were used at dilutions 1:800, 1:400, 1:200, or 1:100 (Figure A3).

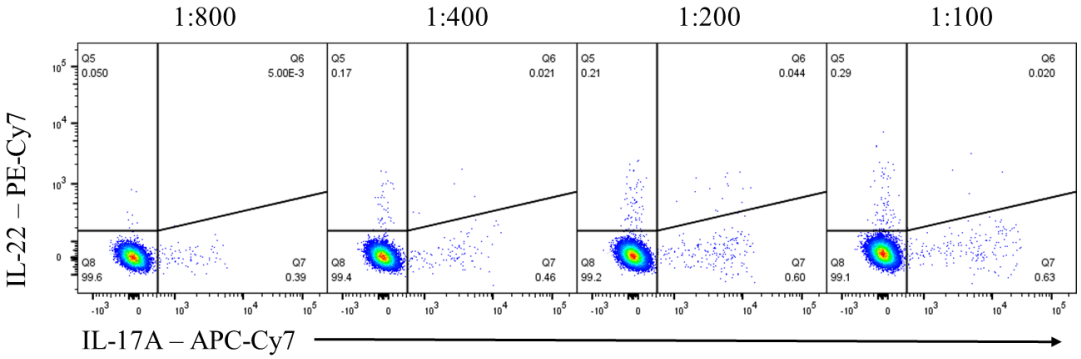

Figure A3. PBMCs were stimulated with PMA/ionomycin as described. Cells were then stained for IL-17A and IL-22 at dilutions of either 1:800, 1:400, 1:200, or 1:100 and analyzed by flow cytometry. Displayed are $CD4^+$ T cells.

An antibody dilution of 1:100 was selected for both IL-17A and IL-22. At this dilution, there was maximum detection of positive staining cells.

KIR3DL1/DS1. The KIR gene region is variable between individuals allowing for numerous possible haplotypes. At the same locus, individuals can contain the allele for KIR3DL1, KIR3DS1, neither, or both.[20] Because of the differing functions between KIR3DL1 and KIR3DS1, it is necessary to be able to differentiate them. However, a flow cytometry antibody specific for KIR3DS1 is not available. The Z27 antibody recognizes both KIR3DL1 and KIR3DS1.[20] When used in conjunction with DX9, an antibody specific for KIR3DL1, it is possible to identify KIR3DS1 cells as Z27 positive but DX9

negative.[20] We tested various dilutions of Z27 and DX9 on PBMCs from a donor known to be heterozygous for KIR3DL1 and KIR3DS1. We titrated the dilutions to optimize the recognition of cells expressing KIR3DL1 or KIR3DS1 (Figure A4).

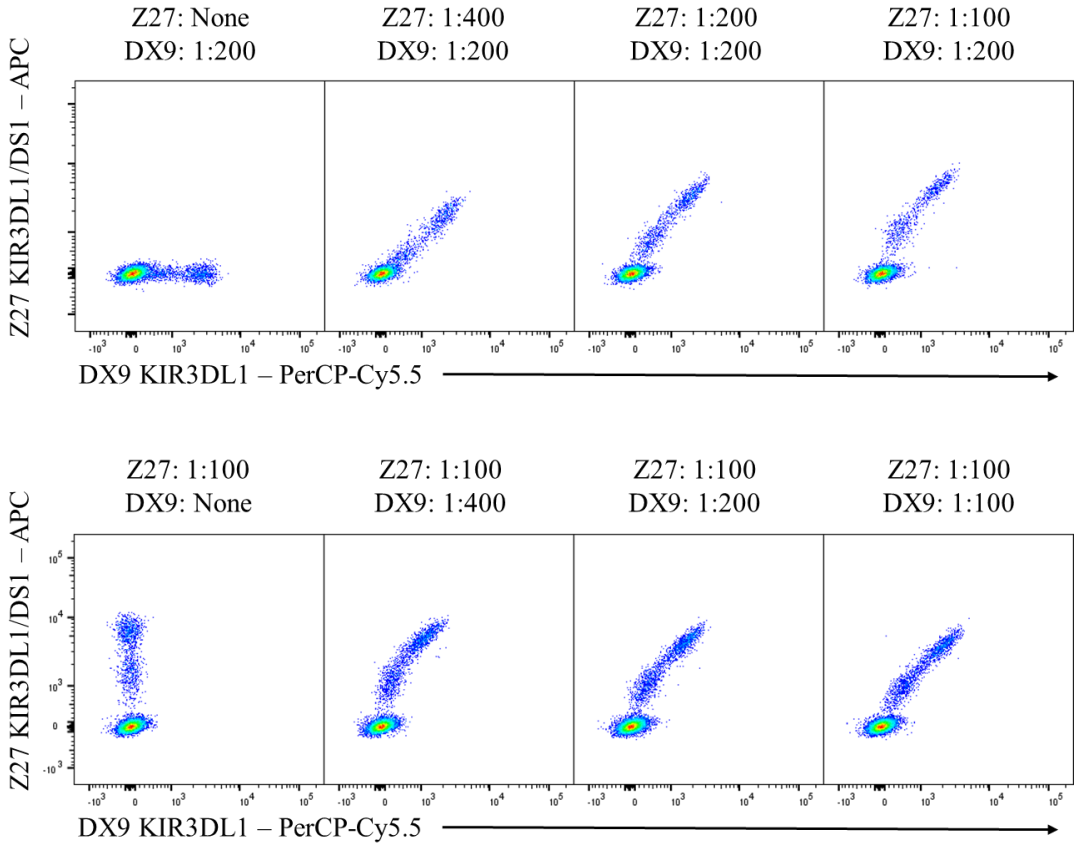

Figure A4. PBMCs were stained with varying concentrations of the DX9 and Z27 antibody clones. Cells were analyzed by flow cytometry and gated using the strategy described in Figure 2. **Top:** NK cells stained with increasing concentration of Z27, DX9 held at 1:200. **Bottom:** NK cells stained with increasing concentrations of DX9, Z27 held at 1:100

Based on these results, we decided to use Z27 at 1:100 and DX9 at 1:400 as it provided the clearest distinctions between the KIR3DL1 and KIR3DS1 populations.

Incubation Medium Selection

One of the primary methods for studying T cell function is to stimulate the cells with PMA and ionomycin.[22] PMA activates protein kinase C while ionomycin is an ionophore that increases cytoplasmic Ca^{2+} concentration.[22] PMA/ionomycin stimulation is thought to mimic T cell receptor activation. RPMI has traditionally been used as the primary medium for T cell incubation in vitro. However, two recent studies demonstrated that T cell activation in IMDM enhances cytokine production, in particular of IL-17A.[21,22] This has been attributed to higher concentration of calcium or aromatic amino acids in IMDM compared to RPMI.[21,22]

Calcineurin is a calcium dependent protein phosphatase that promotes T cell activation.[22] Calcineurin dephosphorylates nuclear factor of activated T cell (NFAT) which enables NFAT to translocate to the nucleus.[22] Once in the nucleus, NFAT induces the transcription of imprinted genes leading to the production of numerous cytokines, such as IL-17A.[22] Another driver of IL-17A production is the aryl hydrocarbon receptor (AhR).[21] AhR binds to numerous ligands including the amino acids phenylalanine, tryptophan, tyrosine, and histidine.[21] When stimulated, AhR serves as a transcription factor that promotes $CD4^+$ T cells to differentiate into Th17 cells and produce IL-17A.[21]

Using PBMCs from 4 different donors, we compared the fraction of cytokine producing cells incubated in IMDM compared to cells incubated RPMI. Following stimulation, cells were stained for flow cytometry analysis including intracellularly for IL-17A, IL-22, IFNγ, and GM-CSF. Fractions of cytokine producing lymphocytes were measured with FlowJo (Figure A5).

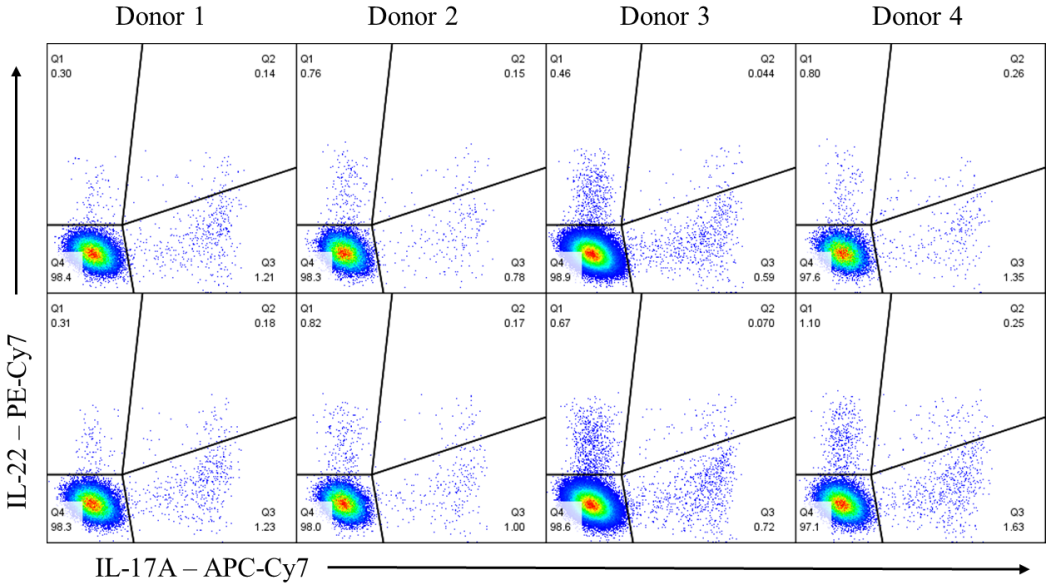

Figure A5. PBMCs from 4 different donors were incubated with PMA/ionomycin in either RPMI-C (top row) or IMDM-C (bottom row) for 4 hours and then analyzed by flow cytometry. Displayed are $CD4^+$ T cells stained for IL-17A and IL-22. PBMCs incubated in IMDM-C had a higher fraction of cytokine induction.

We found that a significantly higher fraction of cells incubated in IMDM during stimulation were positive for IL-17A ($p = 0.0069$) and IL-22, ($p = 0.0425$) (Figure A6).

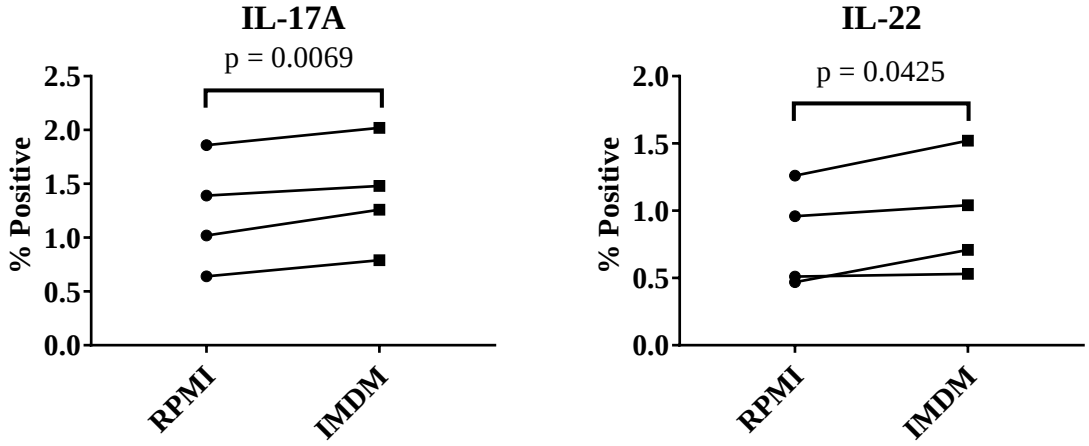

Figure A6. Fraction of IL-17A (left) and IL-22 (right) positive $CD4^+$ T cells from 4 different donors incubated in either RPMI-C or IMDM-C during stimulation with PMA/ionomycin.

Cryopreservation

One limiting factor in studying SpA pathology is collecting tissue from a sufficient number of donors. Our current method of acquiring specimens relies on coordinating with spinal surgeons at multiple clinical sites. Because the prerequisite surgery occurs sporadically, we needed a method of preserving cells while collection occurred so as samples could be analyzed consistently at a central location. We adapted a protocol, previously shown to maintain viability of synovial tissue, to use with ligament and bone tissue.[3] To ensure that cryopreservation did not alter lymphocyte subpopulation proportions or cell phenotype, we compared the profile of lymphocytes isolated from spine tissue processed immediately to tissue that underwent cryopreservation.

Following laminectomy surgery, spinous process bone was cut as described above. Three samples of bone from a single donor were analyzed immediately while another three samples from the same donor were frozen with the method described above and stored at -80° C for 14 days. Lymphocytes from the fresh and cryopreserved tissue were isolated and stained for flow cytometry (Figure A7). No significant change, using a two-tailed student's *t* test, in lymphocyte subset proportions occurred as a result of the cryopreservation (Figure A8).

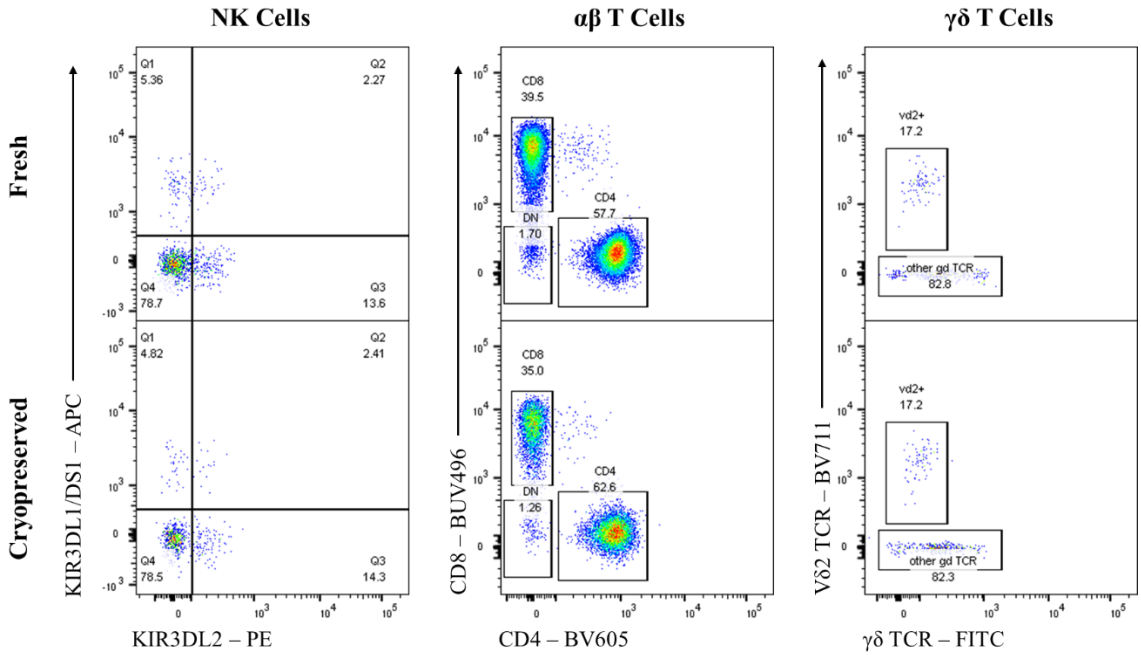

Figure A7. Spinous process bone was either analyzed immediately or stored at -80° C for 14 days. Lymphocytes were isolated using digestion protocol described in methods and analyzed by flow cytometry. Lymphocyte populations were gated on using described strategy. No changes in fluorescent staining occurred as a result of the cryopreservation.

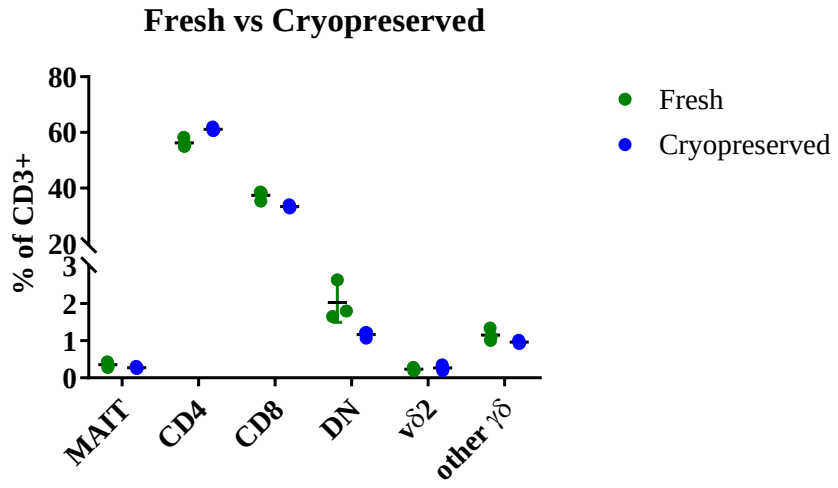

Figure A8. Comparison of spinous process bone from a single donor that was either analyzed immediately or stored at -80° C for 14 days. Three samples of bone of both fresh and cryopreserved tissue were processed. Lymphocytes were isolated using digestion protocol described in methods and analyzed by flow cytometry. Lymphocyte populations were gated on using described strategy. There was no change in lymphocyte population fractions as result of cryopreservation.

Stimulation of Lymphocytes Incubated in Digestive Enzymes

Enzymatic digestion of connective tissue is necessary to isolate lymphocytes from spinal tissue. As shown above, incubating cells in digestive enzymes causes clear alterations in their surface proteins. In order to determine if the process of digestion also has an effect on lymphocyte's capability to produce cytokines, we compared fractions of cytokine positive PBMCs, stimulated with PMA/ionomycin, that were incubated in the digestive enzymes to a matched control. None of the lymphocyte subsets we looked at demonstrated a change in cytokine production (Figure A9 and A10).

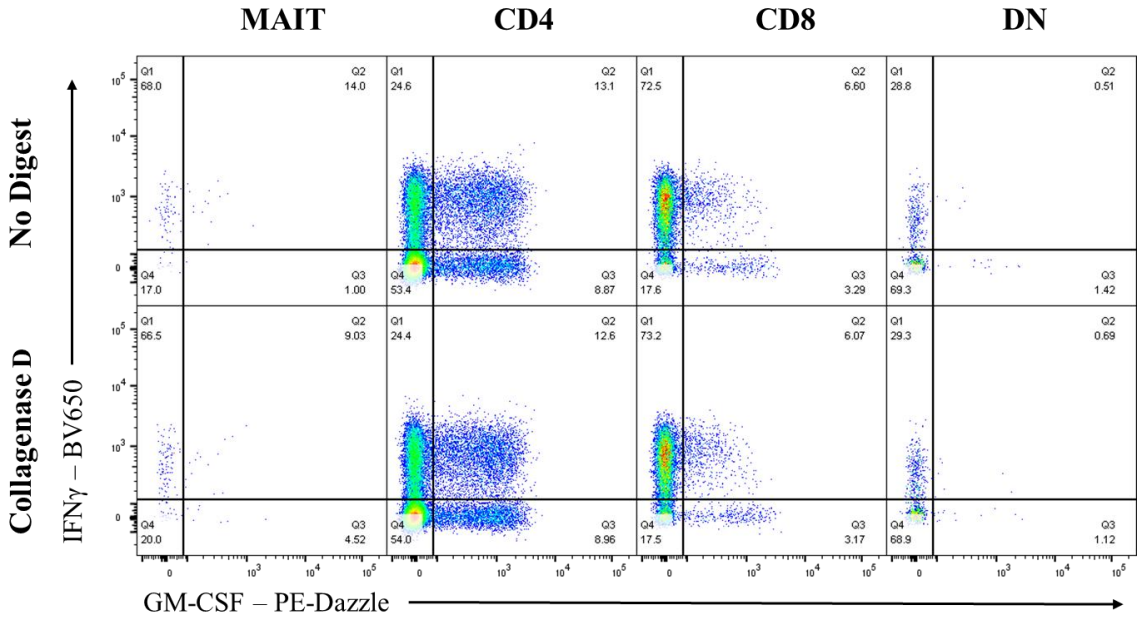

Figure A9. PBMCs were incubated with or without collagenase D for 40 minutes at 37° C. Cells were then stimulated with PMA/ionomycin for 4 hours at 37° C and then analyzed by flow cytometry. Displayed are αβ T cell subsets stained for IFNγ and GM-CSF. No change in cytokine induction occurred as a result of the digestion.

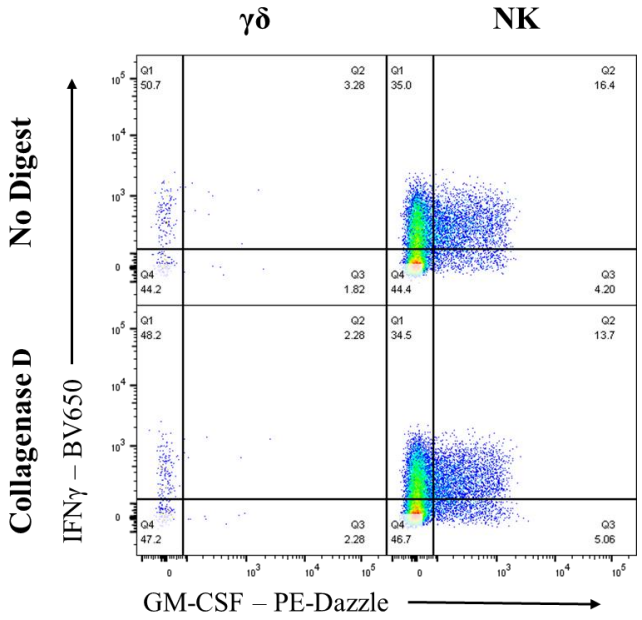

Figure A10. PBMCs were incubated with or without collagenase D for 40 minutes at 37° C. Cells were then stimulated with PMA/ionomycin for 4 hours at 37° C and then analyzed by flow cytometry. Displayed are γδ T cells and NK cells stained for IFNγ and GM-CSF. No change in cytokine induction occurred as a result of the digestion.

LIST OF JOURNAL ABBREVIATIONS

Ann Clin Biochem	Annals of Clinical Biochemistry
Ann Rheum Dis	Annals of the Rheumatic Diseases
Annu Rev Immunol	Annual Review of Immunology
Arthritis Care Res	Arthritis Care and Research
Arthritis Res Ther	Arthritis Research and Therapy
Arthritis Rheum	Arthritis and Rheumatism
Arthritis Rheumatol	Arthritis and Rheumatology
BMJ Open	British Medical Journal Open
Cell Res	Cell Research
Curr Opin Rheumatol	Current Opinion in Rheumatology
Eur J Immunol	European Journal of Immunology
J Exp Med	Journal of Experimental Medicine
Mol Immunol	Molecular Immunology
Nat Med	Nature Medicine
Nat Rev Dis Primer	Nature Reviews Disease Primers
Nat Rev Rheumatol	Nature Reviews Rheumatology
Rheumatol Int	Rheumatology International

REFERENCES

1. Chan AT, Kollnberger SD, Wedderburn LR, Bowness P. Expansion and enhanced survival of natural killer cells expressing the killer immunoglobulin-like receptor KIR3DL2 in spondylarthritis. *Arthritis Rheum*. 2005;52(11):3586-3595. doi:10.1002/art.21395.

2. Cuthbert, Richard J., Fragkakis, Evangelos M., Dunsmuir, Robert, et al. Brief Report: Group 3 Innate Lymphoid Cells in Human Enthesis. *Arthritis Rheumatol*. 2017;69(9):1816-1822. doi:10.1002/art.40150.

3. Donlin LT, Rao DA, Wei K, et al. Methods for high-dimensional analysis of cells dissociated from cryopreserved synovial tissue. *Arthritis Res Ther*. 2018;20(1):139. doi:10.1186/s13075-018-1631-y.

4. Feldtkeller E, Khan M, van der Heijde D, van der Linden S, Braun J. Age at disease onset and diagnosis delay in HLA-B27 negative vs. positive patients with ankylosing spondylitis. *Rheumatol Int*. 2003;23(2):61-66. doi:10.1007/s00296-002-0237-4.

5. Haroon NN, Paterson JM, Li P, Haroon N. Increasing proportion of female patients with ankylosing spondylitis: a population-based study of trends in the incidence and prevalence of AS. *BMJ Open*. 2014;4(12):e006634. doi:10.1136/bmjopen-2014-006634.

6. Ivanov II, McKenzie BS, Zhou L, et al. The Orphan Nuclear Receptor RORγt Directs the Differentiation Program of Proinflammatory IL-17+ T Helper Cells. *Cell*. 2006;126(6):1121-1133. doi:10.1016/j.cell.2006.07.035.

7. Kuijpers TW, Vendelbosch S, Berg M van den, Baeten DLP. Killer immunoglobulin receptor genes in spondyloarthritis: *Curr Opin Rheumatol*. 2016;28(4):368-375. doi:10.1097/BOR.0000000000000302.

8. Lanier LL. Nk Cell Recognition. *Annu Rev Immunol*. 2005;23(1):225-274. doi:10.1146/annurev.immunol.23.021704.115526.

9. Lubberts E. The IL-23–IL-17 axis in inflammatory arthritis. *Nat Rev Rheumatol*. 2015;11(7):415-429. doi:10.1038/nrrheum.2015.53.

10. Maciorowski Z, Chattopadhyay PK, Jain P. Basic Multicolor Flow Cytometry: Basic Multicolor Flow Cytometry. In: Coligan JE, Bierer BE, Margulies DH, Shevach EM, Strober W, eds. *Current Protocols in Immunology*. Hoboken, NJ, USA: John Wiley & Sons, Inc.; 2017:5.4.1-5.4.38. doi:10.1002/cpim.26.

11. McGonagle D, Gibbon W, Emery P. Classification of inflammatory arthritis by enthesitis. *The Lancet*. 1998;352(9134):1137-1140. doi:10.1016/S0140-6736(97)12004-9.

12. Ranganathan V, Gracey E, Brown MA, Inman RD, Haroon N. Pathogenesis of ankylosing spondylitis — recent advances and future directions. *Nat Rev Rheumatol*. 2017;13(6):359-367. doi:10.1038/nrrheum.2017.56.

13. Reveille JD, Witter JP, Weisman MH. Prevalence of Axial Spondylarthritis in the United States: Estimates From a Cross-Sectional Survey. *Arthritis Care Res*. 2012;64(6):905-910. doi:10.1002/acr.21621.

14. Ridley A, Hatano H, Wong-Baeza I, et al. Activation-Induced Killer Cell Immunoglobulin-like Receptor 3DL2 Binding to HLA–B27 Licenses Pathogenic T Cell Differentiation in Spondyloarthritis. *Arthritis Rheumatol*. 2016;68(4):901-914. doi:10.1002/art.39515.

15. Robinson PC, Brown MA. Genetics of ankylosing spondylitis. *Mol Immunol*. 2014;57(1):2-11. doi:10.1016/j.molimm.2013.06.013.

16. Sherlock JP, Joyce-Shaikh B, Turner SP, et al. IL-23 induces spondyloarthropathy by acting on ROR-γt+ CD3+CD4−CD8− entheseal resident T cells. *Nat Med*. 2012;18(7):1069-1076. doi:10.1038/nm.2817.

17. Shi Y, Liu CH, Roberts AI, et al. Granulocyte-macrophage colony-stimulating factor (GM-CSF) and T-cell responses: what we do and don't know. *Cell Res*. 2006;16(2):126-133. doi:10.1038/sj.cr.7310017.

18. Sieper J, Braun J, Dougados M, Baeten D. Axial spondyloarthritis. *Nat Rev Dis Primer*. 2015;1:15013. doi:10.1038/nrdp.2015.13.

19. Sieper J, Rudwaleit M, Baraliakos X, et al. The Assessment of SpondyloArthritis international Society (ASAS) handbook: a guide to assess spondyloarthritis. *Ann Rheum Dis*. 2009;68(Suppl 2):ii1-ii44. doi:10.1136/ard.2008.104018.

20. Trundley A, Frebel H, Jones D, Chang C, Trowsdale J. Allelic expression patterns of KIR3DS1 and 3DL1 using the Z27 and DX9 antibodies. *Eur J Immunol*. 2007;37(3):780-787. doi:10.1002/eji.200636773.

21. Veldhoen M, Hirota K, Christensen J, O'Garra A, Stockinger B. Natural agonists for aryl hydrocarbon receptor in culture medium are essential for optimal differentiation of Th17 T cells. *J Exp Med*. 2009;206(1):43-49. doi:10.1084/jem.20081438.

22. Zimmermann J, Radbruch A, Chang H-D. A Ca2+ concentration of 1.5 mM, as present in IMDM but not in RPMI, is critical for maximal response of Th cells to PMA/ionomycin. *Eur J Immunol*. 2015;45(4):1270-1273. doi:10.1002/eji.201445247.

CURRICULUM VITAE